Konrad-Zuse-Zentrum für Informationstechnik Berlin
Heilbronner Str. 10, D-10711 Berlin - Wilmersdorf

Frank Schmidt David Yevick *

Discrete Transparent Boundary Conditions for Schrödinger-Type Equations

* Queen's University
Department of Electrical Engineering
Kingston, Ontario
CANADA K7L 3N6

Preprint SC 96-17 (May 1996)

Discrete Transparent Boundary Conditions for Schrödinger-Type Equations

Frank Schmidt David Yevick

Contents

Abstract

We present a general technique for constructing nonlocal transparent boundary conditions for one-dimensional Schrödinger-type equations. Our method supplies boundary conditions for the θ-family of implicit one-step discretizations of Schrödinger's equation in time. The use of Mikusiński's operator approach in time avoids direct and inverse transforms between time and frequency domains and thus implements the boundary conditions in a direct manner.

1 Introduction

This paper is concerned with the construction of transparent boundary conditions for evolution partial differential equations of the type

$$\begin{aligned}\partial_t u &= -\frac{i}{c}\left(\partial_x^2 u + V(x,t)u\right), \quad x \in \mathbf{R},\, t > 0 \\ u(x,0) &= u_0\,.\end{aligned} \tag{1}$$

Here c is a real constant and $V(x,t)$ denotes the potential to be specified later. Prototypes of this equation are the Schrödinger equation for an electron with mass m_0

$$i\hbar\partial_t\Psi = -\frac{\hbar^2}{2m_0}\partial_x^2\Psi + V(x,t)\Psi$$

and Fresnel's equation for the evolution of an paraxial electrical field E along the z-direction in a Cartesian coordinate system

$$2in_0k_0\partial_z E = \partial_x^2 E + \left(n^2(x) - n_0^2\right)k_0^2 E\,.$$

The evolution equation (1) is defined in the infinite domain $\Omega = \{x, t \in \mathbf{R} \mid t > 0\}$, where the physical boundary conditions are imposed. For example, if $u_0(x)$ has support only in a finite interval and $\|u_0(x)\|_{L^2}$ is bounded, we expect that $u(x,t)$ must vanish if $x \to \pm\infty$ at any time $t > 0$. For practical purposes, however, the required computational effort is limited by the fact that we wish to compute the solution of (1) only in a finite sub-domain of Ω in order to examine the time evolution in the surrounding of a specified object. In our 1D-case, we accordingly separate the infinite domain Ω into three slab-like parts: an interior domain of finite thickness $\Omega_{\mathrm{i}} = \{x, t \in \mathbf{R} \mid x_{\mathrm{l}} \le x \le x_{\mathrm{r}}\,,\ t > 0\}$ containing the physically relevant part of the solution and two neighboring slabs of infinite thickness $\Omega_{\mathrm{l}} = \{x, t \in \mathbf{R} \mid x \le x_{\mathrm{l}}\,,\ t > 0\}$ and $\Omega_{\mathrm{r}} = \{x, t \in \mathbf{R} \mid x \ge x_{\mathrm{r}}\,,\ t > 0\}$. The general question is then how to transform the zero-boundary conditions at infinity to the boundary conditions at the boundaries of the interior domain.

There are a large number of methods for constructing such boundary conditions, a few of which are discussed below. The methods can be grouped into two classes:

Artificially absorbing layers. One set of simple but powerful boundary conditions continuously modify the potential functions in the exterior domain in order to simulate a physical absorber. The parameters have to be adjusted such that backward diffraction from the absorber is small over a prescribed spectral range (e. g. Kosloff and Kosloff [6] or Yevick [9]. The main advantage of such an approach, as has been remarked by a large number of authors, is its simplicity for two and three-dimensional problems.

Approximate solutions in the entire physical domain. A second class of methods is obtained by analytically constructing boundary conditions in such a manner that the solutions in the interior domain approximate as accurately as possible the whole-space solution of the evolution equation. Following the pioneering work of ENGQUIST and MAJDA [3] on hyperbolic equations, a number of approximation techniques have been proposed for mixed parabolic-hyperbolic systems (HALPERN, [4]) or parabolic equations (HAGSTROM, [5]). In these papers, by Laplace transforming in time the partial differential equation is converted to an second-order ordinary differential equation, which is then solved allowing only for decaying modes in the exterior domains. After transforming into the time-domain the resulting transparent boundary conditions in general become nonlocal in time but are local in space. Computationally advantageous approximations that require little additional computational effort are then obtained by applying a rational approximation to the dispersion relation in the dual frequency domain.

However, for problems in which minimizing the magnitude of the reflected field is more important than computational cost, nonlocal boundary conditions are generally advantageous. The two main categories of nonlocal conditions are, first, methods in which the continuous problem is solved first and then discretized with respect to time, as suggested by BASKAKOV and POPOV [2]. However, such approaches may lead to numerical instabilities. Alternatively, the analytical problem can be consistently formulated for discrete time. In this manner, ARNOLD[1] compose a boundary condition which incorporates both a uniform space and a uniform time discretization. In contrast, the approach by SCHMIDT and DEUFLHARD [8] supposes a given, possibly nonuniform, time-discretization and solves the related exterior ordinary differential equations in the spatial domain with the aid of the Laplace transform. We will label this approach the semi-discrete method. The advantage of the latter procedure is that the exterior space problem is solved exactly and independently of the solution method for the inner problem. Accordingly, the formalism may be easily extended to non-uniform interior discretizations and adaptive methods. On the other hand, Arnold's technique should generally be advantageous in simulations of wave propagations on uniform grids since reflections due to space-discretization effects are fully eliminated.

In this paper we demonstrate that the semi-discrete approach can encompass a uniform time-discretization in a consistent fashion, generating a simple, yet highly-accurate transparent boundary condition. Further we show that this approach may similarly be extended to a uniform space-discretization of the exterior domain and thus to the full discrete case. Our procedure employs both Laplace and Z-transforms in the space variable (and not in time) and the MIKUSIŃSKI representation [7] of the time-discrete problem. We can accordingly construct the desired boundary conditions directly without transforming from the dual to the original domain.

In our analysis, we assume the following two properties of the domain decomposition and the potential function.

- u_0 is supported in Ω_i
- $V(x,t) = \mathrm{const}$ for $(x,t) \in \Omega_\mathrm{l}$ and for $(x,t) \in \Omega_r$,

While the first of these conditions is not required, it significantly simplifies the analysis by allowing us to assume the asymptotic behavior $u(x,t) \to 0$ if $x \to \pm\infty$ for any time $t > 0$. The second condition, which can in fact be replaced by the weaker form $V(x,t) = V(t)$ as in [8], is satisifed by many practical problems and thus has similarly been chosen to permit a compact solution. Let us rewrite (1) as

$$\begin{aligned} \partial_t u &= f(u,t)\ ,\ (x,t) \in \Omega \\ \lim_{x\to\pm\infty} u(x,t) &= 0\,. \end{aligned}$$

To solve this equation numerically, we apply the implicit one-step discretization method

$$\begin{aligned} u_{i+1} - u_i &= \tau f\left(\theta u_{i+1} + (1-\theta)u_i, t_i + \theta\tau\right) \\ \tau &= t_{i+1} - t_i\ , \quad i = 0, 1, \ldots \\ 0 &< \theta \leq 1\,. \end{aligned}$$

Using the definition of $f(u,t)$ from (1), we obtain

$$u_{i+1} - u_i = -i\frac{\tau}{c}\left((\partial_x^2 + V)(\theta u_{i+1} + (1-\theta)u_i)\right). \tag{2}$$

The notation above will be particularly useful in our later implementation and stability analysis of the transparent boundary conditions in § 3.3 and § 3.4. However, for constructing transparent boundary conditions, the following sequence of ordinary differential equations resulting from the time-discretization of the underlying partial differential equation, is more convenient:

$$\begin{aligned} \partial_x^2 u_{i+1} - \lambda^2 u_{i+1} &= -\Theta\partial_x^2 u_i + \kappa^2 u_i\,. \qquad (3) \\ \Theta &= \frac{1-\theta}{\theta} \\ \lambda^2(x, t_i + \theta\tau) &= \frac{ic}{\tau\theta} - V(x, t_i + \theta\tau) \\ \kappa^2(x, t_i + \theta\tau) &= -\frac{ic}{\tau\theta} - \Theta V(x, t_i + \theta\tau)\,. \end{aligned}$$

We now seek solutions u_i, $i \geq 1$ of (3) that vanish at infinity. While we will eventually employ a discretization such as a finite-difference or finite-element representation to solve the interior problem, we focus here on obtaining an exterior solution which enables the boundary conditions to be constructed. For this purpose, we fix the right boundary at $x_\mathrm{r} = 0$, $t > 0$ and search for solutions $u_i(x)$, $i \geq 1$, $x \geq 0$ in the right exterior domain.

2 Preliminary consideration

We first consider the solution, $u_1(x)$, of Eq.(1) in the exterior domain, $x \geq 0$, at the initial time step. This solution is obtained by solving

$$\partial_x^2 u_1 - \lambda^2 u_1 = 0\,,$$

which yields

$$\begin{aligned} u_1(x) &= c_1 \exp(\lambda x) + c_2 \exp(-\lambda x) \\ \text{where} \quad \lambda &= \sqrt{\lambda^2},\ \Re(\lambda) > 0\,. \end{aligned}$$

To satisfy the zero-boundary-condition at infinity, the values of $u_1(0)$ and $\partial_x u_1|_0$ must insure that $c_1 = 0$, leading to the desired form of the solution:

$$u_1(x) = u_1(0) \exp(-\lambda x)\,. \tag{4}$$

This yields the required transformation of the boundary conditions at infinity to the boundary condition at x_r for the first time step. By induction, representing each $u_i(x)$ by a convolution of the homogeneous part of the solution of (3) with the right-hand side of (3) we derive that the general exterior solution can be written as

$$u_i(x) = \sum_{j=1}^{i} P_{j-1}(x) \exp(-\lambda x)\,, \tag{5}$$

where $P_{j-1}(x)$ denotes a polynomial in x of degree $j-1$. The correct asymptotic behavior at large distances is now obtained if the boundary conditions at $x = 0$ are chosen such that

$$\Re(\lambda) > 0\,. \tag{6}$$

The asymptotic form of u_i may be conveniently analyzed by regarding the Laplace transform

$$U_i(p) = \mathcal{L} u_i(x) = \int_0^\infty \mathrm{e}^{-px} u_i(x)\, dx\,.$$

Since the Laplace transform of each term in (5) follows from

$$\mathcal{L}\left\{\frac{x^n}{n!}\mathrm{e}^{-\lambda x}\right\} = \frac{1}{(p+\lambda_j)^{(n+1)}}\,,$$

we can reformulate the condition (6) as

$$U_i(p) < \infty \quad \text{for all } p \text{ with } \Re(p) \geq 0\,, \tag{7}$$

which insures that $U_i(p)$ is bounded in the whole right half-plane. Thus, in order to verify the condition (7) for any time-step, we must analyze the sequence $U_1(p), \ldots, U_{i+1}(p)$ (where the index here refers to the the propagation step number) of Laplace-transformed solutions in the exterior domain. The recurrence relation for this sequence is given directly by the Laplace transformation of (3); namely,

$$U_{i+1} = \frac{p u_{i+1}(0) + \partial_x u_{i+1}|_{x=0} + \Theta(p u_i(0) + \partial_x u_i|_{x=0}) - (\Theta p^2 - \kappa^2) U_i}{p^2 - \lambda^2}\,. \tag{8}$$

To verify the condition (7), we investigate the poles of $U_{i+1}(p)$ in the right half-plane. We express each $U_i(p)$ as quotient of two polynomials. Since $U_1(p)$, given according to (4) by

$$U_1(p) = \frac{u_1(0)}{p+\lambda} \,,$$

has the form $U_1(p) = P_1(p)/Q_1(p)$, we may assume that each $U_i(p)$ possesses the same structure, that is,

$$U_i(p) = \frac{P_i(p)}{Q_i(p)} \,, \quad P_i(p),\, Q_i(p) \text{ - polynomials} \,.$$

From (8) we then obtain

$$U_{i+1}(p) = \frac{\tilde{P}_{i+1}(p)}{(p^2-\lambda^2)Q_i} \,, \tag{9}$$

where $\tilde{P}_{i+1}(p)$ is an as yet undetermined polynomial. However, the above expression is in general unbounded for $p = \lambda$ and $\Re(\lambda) > 0$. Thus the related solutions u_{i+1} will diverge for $x \to \pm\infty$.

We therefore arrive at the central issue of the paper, namely the specification of appropriate boundary conditions which insure the finiteness of $U_{i+1}(p = \lambda)$ for bounded $U_i(p)$ in the right half-plane. That is, we wish to combine $u_{i+1}(0)$ and $\partial_x u_{i+1}|_0$ in $\tilde{P}_{i+1}(p)$, in such a manner that

$$\tilde{P}_{i+1}(\lambda) = 0 \,. \tag{10}$$

As can easily be verified, the two free coefficients associated with the boundary value and the normal derivative) can be combined in such a manner that the result factors as

$$\tilde{P}_{i+1}(p) = (p-\lambda)P_{i+1}(p) \,.$$

This leads to a rational expression for $U_{i+1}(p)$ given by

$$\begin{aligned} U_{i+1}(p) &= \frac{(p-\lambda)P_{i+1}(p)}{(p-\lambda)(p+\lambda)Q_i(p)} \\ &= \frac{P_{i+1}(p)}{Q_{i+1}(p)} \,, \end{aligned}$$

and therefore to a polynomial Q_{i+1}, which does not contain zeros in the right half-plane if such zeros are absent in Q_i. Hence the solution $u_{i+1}(x)$ corresponding to Q_{i+1} possesses the required asymptotic behavior.

3 Operator Formulation

We now formalize the above approach in such a manner that the desired boundary condition is automatically satisfied at each propagation step. As the method is based on the recursive strategy discussed above, it leads to a compact numerical procedure.

3.1 Reformulation Using the Shift-Operator Technique

We first introduce the shift-operator $s = \exp(-p_\tau \tau)$ with $p_\tau = \frac{\partial}{\partial t}$. In our notation this operator shifts the time index i by one unit

$$u_i(x) = s u_{i+1}(x)\,.$$

Accordingly, by the linearity of the Laplace-transform,

$$U_i(p) = s U_{i+1}(p)\,. \tag{11}$$

The direct application of the shift-operator without transforming the underlying equation into the dual, frequency, domain, is in accordance with the algebraic operator theory of Mikusiński [7]. We then rewrite (8) and (9) as

$$U_{i+1}(p) = \frac{p u_{i+1}(0) + \partial_x u_{i+1}|_0 + \Theta(p u_i(0) + \partial_x u_i|_0)}{p^2 - \lambda^2 + s(\Theta p^2 - \kappa^2)}\,. \tag{12}$$

Evidentially if the denominator of (12) approaches zero, i.e. if the semi-discrete dispersion relation

$$p^2 - \lambda^2 + s(\Theta p^2 - \kappa^2) = 0$$

is fulfilled, the homogeneous solution diverges at infinity unless the numerator simultaneously vanishes. The zeros of p occur at the solutions, $p = p_\pm$, of

$$p^2 = \frac{\lambda^2 + \kappa^2 s}{1 + \Theta s}\,,$$

which yields

$$p_\pm = \pm\lambda\sqrt{\frac{1 + \kappa^2/\lambda^2 s}{1 + \Theta s}}, \quad \Re(\lambda) > 0\,.$$

Therefore, the necessary condition that guarantees the exact solution of (3) is

$$p_+ u_{i+1}(0) + \partial_x u_{i+1}|_{x=0} + \Theta(p_+ u_i(0) + \partial_x u_i|_{x=0}) = 0, \quad i \geq 0\,. \tag{13}$$

The recursive structure of (13) combined with the requirement that $u_0(x) = 0$ for $x \geq 0$, yields finally the following compact form of the desired transparent boundary condition

$$\begin{aligned} p_+ u_{i+1}(0) + \partial_x u_{i+1}|_{x=0} &= 0 & (14)\\ p_+ &= \lambda\sqrt{\frac{1 + \kappa^2/\lambda^2 s}{1 + \Theta s}}, \quad \Re(\lambda) > 0\,. & (15) \end{aligned}$$

For future implementation it is convenient to split p into a s-independent part and a second expression which has the property that each term in its Taylor series representation is homogeneous with respect to s according to

$$\begin{aligned} p_+ &= p_I + p_H \\ p_I &= \lambda \\ p_H(s) &= \lambda\left(-1 + \sqrt{\frac{1 + \kappa^2/\lambda^2 s}{1 + \Theta s}}\right)\,. \end{aligned}$$

This representation enables us to seperate the term corresponding to multiplication by a constant coefficient from terms that generate the index-shifts.

Special case I: implicit midpoint discretization. We now illustrate (14) for potential functions that vanish outside the inner domain Ω_i. Considering first a implicit midpoint discretization for which $\theta = 0.5$ and $\Theta = 1$, we have

$$\begin{aligned} p_+ &= \lambda\sqrt{\frac{1-s}{1+s}} \\ &= \lambda\left(1 - s + \frac{1}{2}s^2 - \frac{1}{2}s^3 + \frac{3}{8}s^4 - \frac{3}{8}s^5 + \ldots\right), \end{aligned} \tag{16}$$

yielding the following boundary condition

$$\lambda u_{i+1} + \partial_x u_{i+1}|_{x=0} = \lambda\left(u_i - \frac{1}{2}u_{i-1} + \frac{1}{2}u_{i-2} - \frac{3}{8}u_{i-3} + \frac{3}{8}u_{i-4} - \ldots\right)\Big|_{x=0}. \tag{17}$$

Special case II: implicit Euler discretization. Considering next the implicit Euler scheme in the propagation direction, we apply instead $\theta = 1$ and $\Theta = 0$. We then obtain in place of Eqs. (16) and (17)

$$\begin{aligned} p_+ &= \lambda\sqrt{1-s} \\ &= \lambda\left(1 - \frac{1}{2}s - \frac{1}{8}s^2 - \frac{1}{16}s^3 - \frac{5}{128}s^4 - \ldots\right), \end{aligned}$$

and

$$\lambda u_{i+1} + \partial_x u_{i+1}|_{x=0} = \lambda\left(\frac{1}{2}u_i + \frac{1}{8}u_{i-1} + \frac{1}{16}u_{i-2} + \frac{5}{128}u_{i-3} + \ldots\right)\Big|_{x=0}.$$

3.2 Finite-Difference Implementation

Having developed the continuous formulation of our transparent boundary condition, we now examine finite-difference and finite-element implementations. Considering first the finite-difference formalism, we wish to transform (3) into its corresponding discrete approximation. That is, we must replace $\partial_x^2 u$ by its discrete analogue on both the right and the left-hand side of (3). In the case of a uniform computational grid with a step-width $x^i - x^{i-1} = h$ for all inner points we substitute in standard fashion

$$\partial_x^2 u\Big|_{x=x^i} \to \frac{1}{h^2}\left(u^{i-1} - 2u^i + u^{i+1}\right)$$

with a $O(h^2)$ discretization error. At the $x = 0$ boundary, however, we instead apply the Taylor expansion of $u(x)$ at $x = 0$,

$$u(h) = u(0) + u'(0)\,h + \frac{1}{2}u''(0)\,h^2 + O(h^3),$$

to rewrite $\partial_x^2 u$ as

$$\partial_x^2 u\Big|_{x=0} = \frac{2}{h^2}\left(u(-h) - u(0) + h\,\partial_x u|_{x=0}\right) + O(h).$$

Here we assume that $u(0), u'(0)$ and the rightmost inner value $u(-h)$ are given. Thus we must rewrite the differential equation, (3), at the boundary in the finite-difference implementation as

$$\left(\partial_x^2 u + \mathrm{const}\, u\right)_{x=0} \to \frac{2}{h^2}\left(u(-h) - u(0) + h\,\partial_x u|_{x=0}\right) + \mathrm{const}\, u(0)\,.$$

The above boundary condition is now substituted for the normal derivative of u, leading to the finite-difference representation of the transparent boundary condition.

3.3 Finite-Element Implementation

Next, we derive and discuss a transparent boundary condition analogous to that of the previous section, but based on a finite-element discretization (14) of (2). The finite-element method automatically satisifies the symmetry properties required for numerical stability. However, many other discretization methods such as the finite-difference approach can be shown to possess identical symmetries and are therefore equally stable. The weak form of (2) is

$$\begin{aligned}(v, u_{i+1}) + i\frac{\tau}{c}\theta\Big(\partial_x u_{i+1}|_{x=x_\mathrm{l}}^{x=x_\mathrm{r}} + a(v, u_{i+1})\Big) = \\ (v, u_i) + i\frac{\tau}{c}(1-\theta)\Big(\partial_x u_i|_{x=x_\mathrm{l}}^{x=x_\mathrm{r}} - a(v, u_i)\Big),\end{aligned} \tag{18}$$

$$\text{with}\quad a(v,u) = -\int \partial_x \bar{v}\partial_x u + \int \bar{v} V(x) u \tag{19}$$

$$(v,u) = \int \bar{v} u \tag{20}$$

for any $v \in H^1(\Omega_\mathrm{i})$. Discretizing the problem restricts the test-function space to $V_h \subset H^1(\Omega_\mathrm{i})$. Accordingly, we obtain the matrices $\mathbf{A}$ and $\mathbf{M}$ from the bilinear forms $a(\cdot,\cdot) \to \mathbf{A}$ and $m(\cdot,\cdot) \to \mathbf{M}$. Hence the discrete version of (20) yields

$$\begin{aligned}\left(\mathbf{M} + i\frac{\tau}{c}\theta\mathbf{A}\right)\mathbf{u}_{i+1} + i\frac{\tau}{c}\theta\begin{pmatrix} -\,\partial_x u_{i+1}|_{x=x_\mathrm{l}} \\ \mathbf{0} \\ \partial_x u_{i+1}|_{x=x_\mathrm{r}}\end{pmatrix} = \\ \left(\mathbf{M} - i\frac{\tau}{c}(1-\theta)\mathbf{A}\right)\mathbf{u}_i - i\frac{\tau}{c}(1-\theta)\begin{pmatrix} -\,\partial_x u_i|_{x=x_\mathrm{l}} \\ \mathbf{0} \\ \partial_x u_i|_{x=x_\mathrm{r}}\end{pmatrix}.\end{aligned}$$

Together with the boundary condition (14), we arrive at the final form of the equation system

$$\left(\mathbf{M}+i\frac{\tau}{c}\theta\mathbf{A}\right)\mathbf{u}_{i+1}-i\frac{\tau}{c}\theta p_I\begin{pmatrix}u_{i+1}(x_{\mathrm{l}})\\ \mathbf{0}\\ u_{i+1}(x_{\mathrm{r}})\end{pmatrix}=\left(\mathbf{M}-i\frac{\tau}{c}(1-\theta)\mathbf{A}\right)\mathbf{u}_i+$$

$$+i\frac{\tau}{c}(1-\theta)(p_+(s))\begin{pmatrix}u_i(x_{\mathrm{l}})\\ \mathbf{0}\\ u_i(x_{\mathrm{r}})\end{pmatrix}+i\frac{\tau}{c}\theta p_H(s)\begin{pmatrix}u_{i+1}(x_{\mathrm{l}})\\ \mathbf{0}\\ u_{i+1}(x_{\mathrm{r}})\end{pmatrix}. \qquad (21)$$

3.4 Stability Properties

We now introduce the notation

$$\langle \mathbf{v},\mathbf{u}\rangle=\bar{\mathbf{v}}^T\mathbf{u}\,,$$

for Euclidean inner product, while the discrete L^2-product in terms of the symmetric positive definite matrix $\mathbf{M}$ defined above is written as

$$\langle \mathbf{v},\mathbf{u}\rangle_{\mathbf{M}}=\bar{\mathbf{v}}^T\mathbf{M}\mathbf{u}\,,$$

and the related discrete L^2-norm is

$$\|\mathbf{u}\|=\sqrt{\langle \mathbf{u},\mathbf{u}\rangle_{\mathbf{M}}}\,.$$

We now show that given matrix $\mathbf{A}$ which is self-adjoint with respect to the Euclidean inner product, for $0.5\le\theta\le 1$ the discrete $L^2(\Omega_{\mathrm{i}})$ norms of $\mathbf{u}_1,\dots,\mathbf{u}_{i+1}$ obtained using (21) remain bounded for any time step τ. Hence our numerical scheme is unconditionally stable under these conditions. To prove our assertion, we again invoke the weak form of (2) that forms the basis of (21). We now however rearrange the expression as follows,

$$\begin{aligned}(v,u_{i+1}-u_i) &= -i\frac{\tau}{c}a\,(v,u_\theta)-i\frac{\tau}{c}\left((\bar v\;\partial_x u_\theta)|_{x=x_{\mathrm{l}}}^{x=x_{\mathrm{r}}}\right) \qquad (22)\\ \text{with}\quad u_\theta &= \theta u_{i+1}+(1-\theta)u_i\,.\end{aligned}$$

Restricting (22) again to its discrete form, setting $v=u_\theta$ and taking the real part yields

$$\Re\langle \mathbf{u}_\theta,\mathbf{u}_{i+1}-\mathbf{u}_i\rangle_{\mathbf{M}}=-\frac{\tau}{c}\Re\left(i(\bar u_\theta\;\partial_x u_\theta)|_{x=x_{\mathrm{l}}}^{x=x_{\mathrm{r}}}\right)\,.$$

A rearrangment of the terms in the above expression leads to

$$\begin{aligned}&\langle \mathbf{u}_{i+1},\mathbf{u}_{i+1}\rangle_{\mathbf{M}}-\langle \mathbf{u}_i,\mathbf{u}_i\rangle_{\mathbf{M}}=\\ &\quad -2(\theta-\frac{1}{2})\langle \mathbf{u}_{i+1}-\mathbf{u}_i,\mathbf{u}_{i+1}-\mathbf{u}_i\rangle_{\mathbf{M}}-2\frac{\tau}{c}\Re\left(i(\bar u_\theta\;\partial_x u_\theta)|_{x=x_{\mathrm{l}}}^{x=x_{\mathrm{r}}}\right)\,.\end{aligned}$$

The same procedure can be applied to the exact solutions of (2) in the exterior regions. For the right exterior domain $x \geq x_\mathrm{r}$

$$
\begin{aligned}
&(u_{i+1}, u_{i+1}) - (u_i, u_i) = \\
&\quad -2(\theta - \frac{1}{2})\,(u_{i+1} - u_i, u_{i+1} - u_i) - 2\frac{\tau}{c}\Re\left(i\,(\bar{u}_\theta\;\partial_x u_\theta)|_{x=x_\mathrm{r}}^{x=\infty}\right)
\end{aligned}
$$

with an analogous result for the left exterior domain. Our boundary conditions however preserve the exponential decay of the exact solution of (2) in the exterior domains as both exterior solutions are described by (5), with $\Re\lambda > 0$. Hence, the boundary terms vanish as $x \to \infty$ and further cancel at $x = x_{\mathrm{l,r}}$ so that

$$
\begin{aligned}
&\sum_{j=\mathrm{l,r}} (u_{i+1}, u_{i+1})_{\Omega_j} + \langle \mathbf{u}_{i+1}, \mathbf{u}_{i+1} \rangle_\mathbf{M} - \left(\sum_{j=\mathrm{l,r}} (u_i, u_i)_{\Omega_j} + \langle \mathbf{u}_i, \mathbf{u}_i \rangle_\mathbf{M} \right) \\
&\quad = \; -2\left(\theta - \frac{1}{2}\right)\left(\sum_{j=\mathrm{l,r}} (u_{i+1} - u_i, u_{i+1} - u_i)_{\Omega_j} + \langle \mathbf{u_{i+1}} - \mathbf{u_i}, \mathbf{u_{i+1}} - \mathbf{u_i} \rangle_\mathbf{M} \right) .
\end{aligned}
$$

The right-hand side of the above expression is non-positive for $\theta \geq 0.5$, establishing both the numerical stability of the algorithm and the uniqueness of the interior solution. Furthermore, for the implicit midpoint rule, $\theta = 0.5$, we find

$$
\sum_{j=\mathrm{l,r}} (u_i, u_i)_{\Omega_j} + \langle \mathbf{u}_i, \mathbf{u}_i \rangle_\mathbf{M} = \text{const for all } i \geq 0\,. \tag{23}
$$

Eq. (23) extends the conservation property of the implicit mid-point rule with homogeneous Dirichlet or Neumann boundary conditions to the entire real space.

4 Discrete Solution of the Exterior Problem

We now consider the case of uniform spatial discretization in the interior domain Ω_i. Under the assumption of a uniform grid point spacing in the exterior domain, an identical finite-difference stencil can be applied in both the interior and exterior domains, providing an approximate solution of the continuous problem. Hence in this particular case, completely reflection-free boundary conditions can be realized by sacrificing the quality of the approximation applied to the exterior domain. In contrast, the semi-discrete approach discussed above supplies the exact solution of (3) in the exterior domain, at the cost of a small residual reflection, which of course vanishes as $h \to 0$. The nature of the residual reflection is evident from a backward analysis of the problem in which the discrete inner solution is considered as the exact solution of a slightly modified equation. Unless the same discrete approximation is employed in the exterior and interior domains, the difference in the underlying equation in the two domains necessarily produces a small reflected field.

4.1 Discrete Treatment of the Space Coordinate

To implement the above procedure, we associate the solution points at the ith propagation step with physical locations according to the formula

$$u_i^{(j)} = u_i(j \cdot h), \quad j \geq -1, \quad i \geq 0 .$$

Here u_i^{-1} is the rightmost inner value in Ω_i while u_i^0 is located on the boundary between the internal and the right external region. The equation corresponding to (12) is obtained by introducing the sequences

$$\begin{aligned} \mathrm{u}_i &= \{u_i^{(0)}, u_i^{(1)}, u_i^{(2)}, \ldots\} \\ \mathrm{u}_i^+ &= \{u_i^{(1)}, u_i^{(2)}, u_i^{(3)}, \ldots\} \\ \mathrm{u}_i^- &= \{u_i^{(-1)}, u_i^{(0)}, u_i^{(1)}, \ldots\} , \end{aligned}$$

with Z-transforms

$$\begin{aligned} \mathcal{U}_i &= \mathcal{Z}\mathrm{u}_i = u_i^{(0)} + \frac{1}{z}u_i^{(1)} + \frac{1}{z^2}u_i^{(2)} + \ldots \\ \mathcal{U}_i^+ &= \mathcal{Z}\mathrm{u}_i^+ = u_i^{(1)} + \frac{1}{z}u_i^{(2)} + \frac{1}{z^2}u_i^{(3)}, \ldots \\ \mathcal{U}_i^- &= \mathcal{Z}\mathrm{u}_i^- = u_i^{(-1)} + \frac{1}{z}u_i^{(0)} + \frac{1}{z^2}u_i^{(1)}, \ldots . \end{aligned}$$

Suppressing the time-step subscript i in the following, we observe next that the transforms $\mathcal{U}^+$ and $\mathcal{U}^-$ are related to $\mathcal{U}$ by

$$\mathcal{U}^- = \frac{1}{z}\mathcal{U} + u^{(-1)} \tag{24}$$

$$\mathcal{U}^+ = z\left(\mathcal{U} - u^{(0)}\right) . \tag{25}$$

If we now Z transform the finite-difference form of (3) in Ω_r,

$$\frac{1}{h^2}\left(u_{i+1}^{j-1} - 2u_{i+1}^j + u_{i+1}^{j+1}\right) - \lambda^2 u_{i+1}^j = -\frac{\Theta}{h^2}\left(u_i^{j-1} - 2u_i^j + u_i^{j+1}\right) + \kappa^2 u_i^j \qquad j \geq -1, \quad i \geq 0$$

we obtain

$$\frac{1}{h^2}\left(\mathcal{U}_{i+1}^- - 2\mathcal{U}_{i+1} + \mathcal{U}_{i+1}^+\right) - \lambda^2\mathcal{U}_{i+1} = -\frac{\Theta}{h^2}\left(\mathcal{U}_i^- - 2\mathcal{U}_i + \mathcal{U}_i^+\right) + \kappa^2\mathcal{U}_i \qquad i \geq 0 .$$

This equation yields, in view of (24) and the shift-operator definition (11),

$$\mathcal{U}_{i+1}(z) = -\frac{u_{i+1}^{(-1)} - zu_{i+1}^{(0)} + \Theta(u_i^{(-1)} - zu_i^{(0)})}{z - (2 + h^2\lambda^2) + \frac{1}{z} + s\Theta\left(z - (2 + h^2\kappa^2/\Theta) + \frac{1}{z}\right)} .$$

Again in analogy to the continuous case, we now compute the zeros $z_{\pm}$ of the discrete dispersion relation

$$z - (2 + h^2\lambda^2) + \frac{1}{z} + s\Theta\left(z - \left(2 + h^2\frac{\kappa^2}{\Theta}\right) + \frac{1}{z}\right) = 0\,, \tag{26}$$

which are given by

$$\begin{aligned} z_{\pm}(s) &= 1 + q_{\pm}(s) && (27)\\ \text{with} \quad q_{\pm}(s) &= c_1\frac{1+\beta^2 s}{1+\Theta s} \pm c_2\sqrt{\frac{1+\beta^2 s}{1+\Theta s}}\sqrt{\frac{1+\gamma^2 s}{1+\Theta s}} && (28)\\ c_1 &= \frac{1}{2}h^2\lambda^2 \\ c_2 &= \frac{1}{2}\sqrt{h^2\lambda^2}\sqrt{4+h^2\lambda^2} \\ \gamma^2 &= \frac{4\Theta + h^2\kappa^2}{4+h^2\lambda^2} \\ \beta^2 &= \frac{\kappa^2}{\lambda^2}\,. \end{aligned}$$

Applying the root-theorem of VIETA to (26) we find $z_+z_- = 1$. If we define z_+ and z_- such that $|z_-| < 1$ and $|z_+| > 1$. Then, choosing the square-roots such that $\Re(c_2) > 0$, the desired discrete counterpart to the transparent boundary condition (14) is given by

$$u_{i+1}^{(-1)} - z_+u_{i+1}^{(0)} = 0\,,$$

or equivalently,

$$u_{i+1}^{(0)} - u_{i+1}^{(-1)} + q_+u_{i+1}^{(0)} = 0\,. \tag{29}$$

4.2 Implementation

To incorporate (29) into a numerical code, we proceed exactly as in § 3.3. In particular, we first derive the equation system for homogeneous Neumann conditions. We set formally $q_+ = 0$ to obtain the equation system

$$\left(\mathbf{M} + i\frac{\tau}{c}\theta\mathbf{A}\right)\mathbf{u}_{i+1} = \left(\mathbf{M} - i\frac{\tau}{c}(1-\theta)\mathbf{A}\right)\mathbf{u}_i, \tag{30}$$

after applying the FD-stencil to all inner points and discretizing the second derivative operator according to

$$\partial_x^2 u|_{x=x_\mathrm{r}} \to \frac{1}{h^2}(u^{-1} - u^0)$$

for the right boundary with an analogous expression at the left boundary. Completing this system by imposing the boundary condition (29) yields

$$\left(\mathbf{M} + i\frac{\tau}{c}\theta\mathbf{A}\right)\mathbf{u}_{i+1} - i\frac{\tau}{ch^2}\theta q_+(s)\begin{pmatrix} u_{i+1}(x_\mathrm{l}) \\ \mathbf{0} \\ u_{i+1}(x_\mathrm{r}) \end{pmatrix} =$$

$$\left(\mathbf{M} - i\frac{\tau}{c}(1-\theta)\mathbf{A}\right)\mathbf{u}_i + i\frac{\tau}{ch^2}(1-\theta)q_+(s)\begin{pmatrix} u_i(x_\mathrm{l}) \\ \mathbf{0} \\ u_i(x_\mathrm{r}) \end{pmatrix}.$$

After the operator q is seperated into its homogeneous and inhomogeneous parts, we finally arrive at

$$\left(\mathbf{M} + i\frac{\tau}{c}\theta\mathbf{A}\right)\mathbf{u}_{i+1} - i\frac{\tau}{ch^2}\theta q_I\begin{pmatrix} u_{i+1}(x_\mathrm{l}) \\ \mathbf{0} \\ u_{i+1}(x_\mathrm{r}) \end{pmatrix} = \left(\mathbf{M} - i\frac{\tau}{c}(1-\theta)\mathbf{A}\right)\mathbf{u}_i +$$

$$+ i\frac{\tau}{ch^2}(1-\theta)q_+(s)\begin{pmatrix} u_i(x_\mathrm{l}) \\ \mathbf{0} \\ u_i(x_\mathrm{r}) \end{pmatrix} + i\frac{\tau}{ch^2}\theta q_H(s)\begin{pmatrix} u_{i+1}(x_\mathrm{l}) \\ \mathbf{0} \\ u_{i+1}(x_\mathrm{r}) \end{pmatrix}.$$

Numerical Stability. As the arguments presented in Sec.3.4 are equally valid for the discrete problem, our implicit one-step methods are unconditionally stable for $0.5 \leq \theta \leq 1$, provided the discretization insures that matrix $\mathbf{M}$ is symmetric positive definite and that the matrix $\mathbf{A}$ is self-adjoint with respect to the Euclidean inner product.

5 Application to the Fresnel Equation

Having outlined both the theory and the implementation of the discrete transparent boundary conditions we now investigate the two test cases of [9] associated with optical beam propagation in the Fresnel approxiation. The first of these involves a single beam with a Gaussian profile $\mathrm{e}^{-x^2/(10\mu m)^2}$ propagating in vacuum, $n = 1$, at a wavelength of $0.832\mu m$ and describing an angle of $\alpha = 21.8^0$ with respect to the z-axis. The computational window has a width of $200\mu m$ while the propagation step length $\Delta z = 0.4\mu m$ and the reference refractive index $n_0 = n\cos\alpha$. The propagation distance of $Z = 500\mu m$ is selected to yield a single reflection from the boundary. A second set of comparisions involves a superposition of two $10\mu m$ Gaussians beams, one displaced a distance $-12.5\mu m$ from the coordinate origin and propagating at an angle of 26.8^0 and the second displaced $+12.5\mu m$ from the coordinate origin and propagating at 16.8^0.

In all test cases a uniform finite-difference discretization in x-direction has been utilized together with the implicit midpoint rule in the direction of propagation (z-axis). In order to visualize the residual reflections the 10^{-10}, 10^{-8}, 10^{-6}, 10^{-4}, 10^{-2},

10^{-1} iso-lines of $|u(x,z)|^2$, where $u(x,z)$ is the numerically calculated electric field profile normalized such that $|u(x,0)| = 1$, are plotted.

Semidiscrete Approach: Fig. 1 displays the iso-line plot for the first test case corresponding to the propagation of a single beam on an uniform $N = 1024$ point transverse grid. As expected from the above theory, some small reflections are produced by the discretization error in the transverse, x, direction. Our simulation

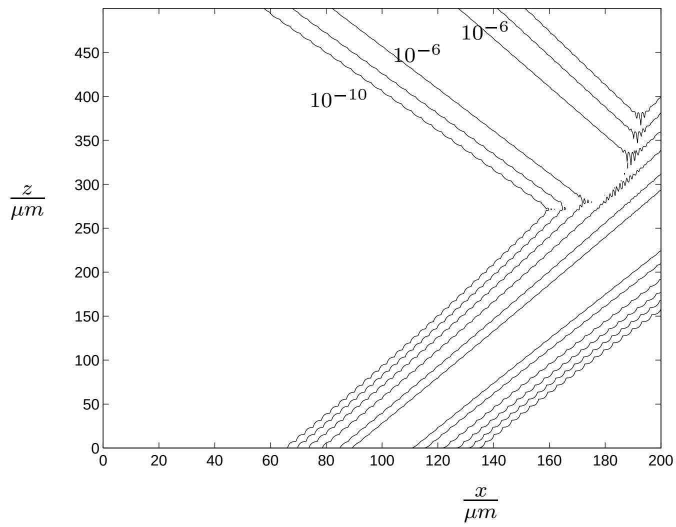

Figure 1: Iso-curves for the electric power for a single Gaussian beam and $N = 1024$ grid points

of the second test example in Fig. 2 supplies similar results. The magnitude of the reflections are approximately the same as in the former case despite the far more complicated shape of the field at the window boundaries.

In order to verify that the magnitude of the reflection depends on the accuracy of the inner solution rather then on the shape of the propagating field, we have repeated our numerical experiments for $N = 8192$ transverse discretization points, generating the results given in Fig. 3 and Fig. 4. It is evident from these figures that the spurious reflections are supressed as the the accuracy of the inner solution increases.

In Fig. 5, we instead present the discrete L^2-norm of the field, $u(x,z)$, remaining inside the computational window as a function of the number of transverse discretization points. The plateaus in the figures indicate the power reflection coefficient after an integer number of reflections. Clearly, these results confirm that magnitude of the reflection coefficient varies with the x-discretization error of the problem in the interior domain.

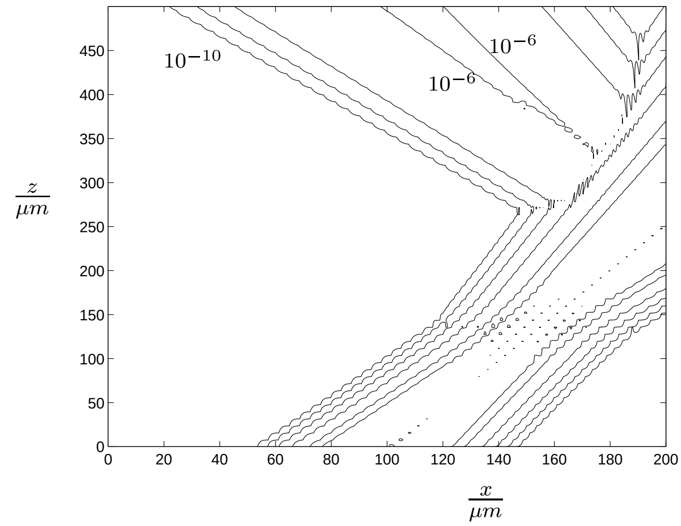

Figure 2: Iso power curves for a two-beam test case with $N = 1024$

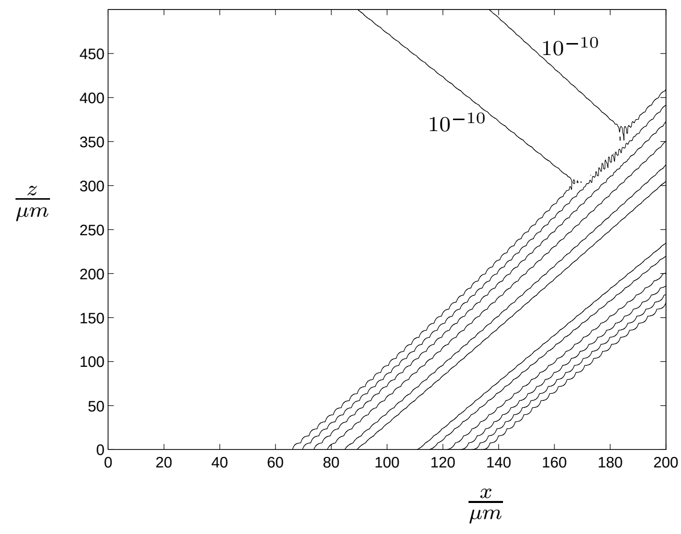

Figure 3: Iso power curves for the single-beam test case with $N = 8192$

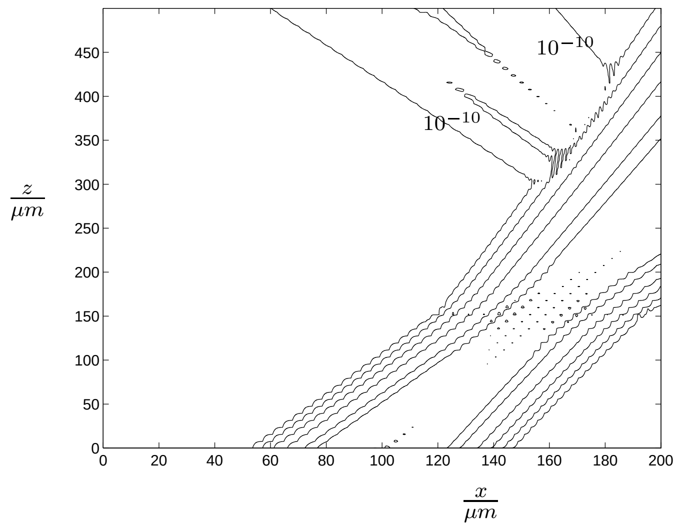

Figure 4: Iso power curves for the two-beam case with $N = 8192$

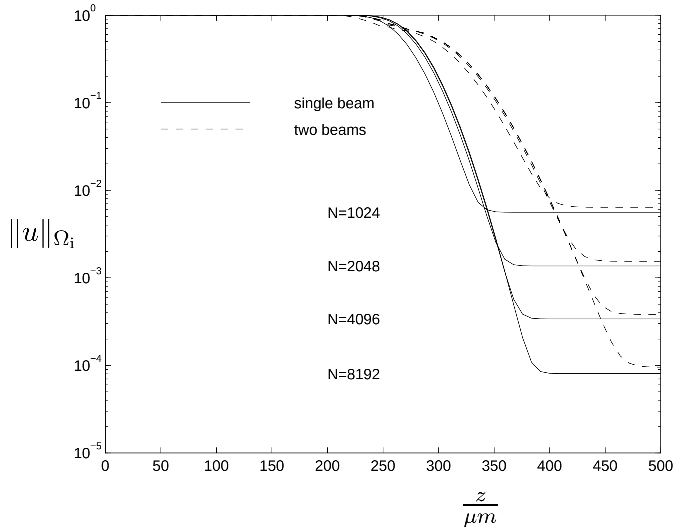

Figure 5: The discrete L^2-norm of the electric field remaining inside the computational window for $N = 8192$

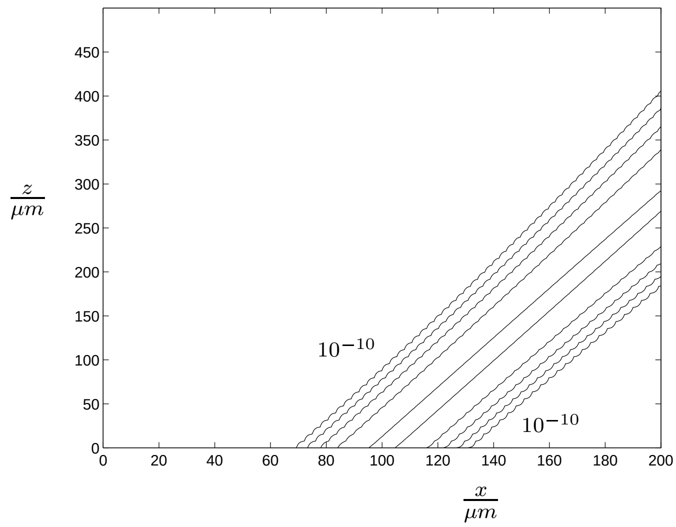

Figure 6: Iso power curves for the single-beam with $N = 1024$ in the full discrete approach

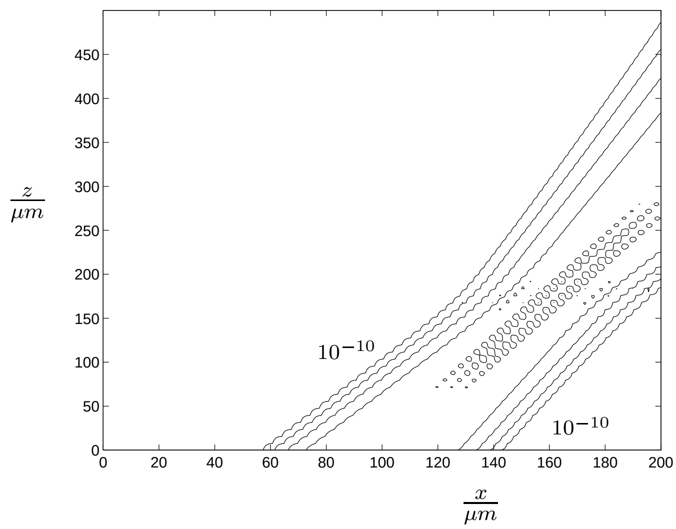

Figure 7: Iso-curves for the two-beam test case with $N = 1024$ in the full discrete approach

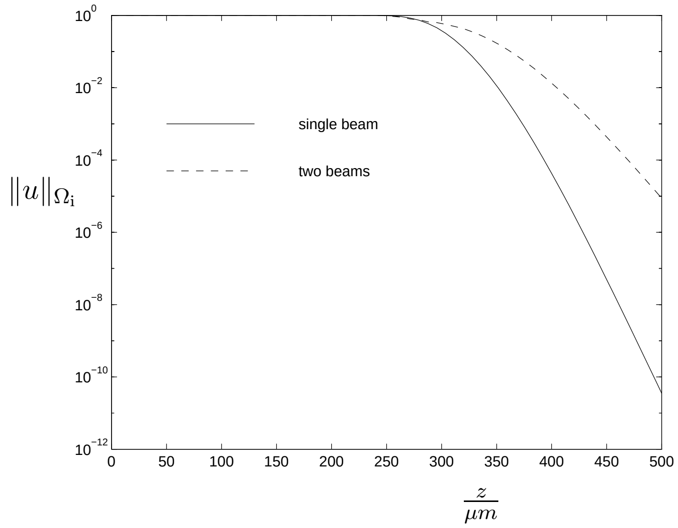

Figure 8: Discrete L^2-norm of the electric field remaining inside the computational window for $N = 1024$

We finally demonstrate that the spurious reflections of the previous examples can be avoided with the aid of our full discrete approach, for uniformly spaced grid points. Repeating our test examples with $N = 1024$ grid points, we thus obtain the iso-lines of Fig.'s 6 and 7 which contain no observable reflected power. The corresponding evolution of the discrete L^2-norm is presented in Fig. 8. We infer from these figures that the full discrete approach is preferable numerically in this special case (uniform meshes) although, as noted above, the quality of the discrete approximation on the exterior domain is reduced in this procedure.

Conclusions

We have constructed general transparent boundary conditions for uniformly discretized 1D Schrödinger-type equations based on a recursive semi-discrete formulation presented in [8]. As our method is derived directly from the MIKUSIŃSKI' operator theory, Z-transforms in the time variable of the field at the boundary are not present. Accordingly, our derivations and formulas are particularly simple in nature, yielding additional insight into the structure and behavior of reflectionless boundary conditions.

Acknowledgements

The authors acknowledge the continuous support and helpful discussions by P. Deuflhard and F. A. Bornemann. One of us (D.Y.) would like to acknowledge support from the the Ontario Centre for Materials Research, Bell Northern Research, Corning Glass, and the National Sciences and Research Council of Canada.

References

[1] A. Arnold: *Numerically Absorbing Boundary Conditions for Quantum Evolution Equations*, Preprint Nr. 481, Department of Mathematics, Technical University Berlin (1995)

[2] V. A. Baskakov, A. V. Popov: *Implementatiom of transparent boundaries for numerical solution of the Schrödinger equation* Wave Motion 14, pp. 123-128, (1991)

[3] B. Engquist, A. Majda: *Absorbing Boundary Conditions for the Numerical Simulation of Waves* Math. Comp. 31, pp. 629-651 (1977)

[4] L. Halpern: *Artificial boundary conditions for incompletely parabolic perturbations of hyperbolic systems*, SIAM J. Math. Anal. 22, 1256-1283 (1991)

[5] T. M. Hagstrom: *Asymptotic expansions and boundary conditions for time-dependent problems*, SIAM J. Num.Anal. 23, 948-958 (1986)

[6] R. Kosloff, D. Kosloff: *Absorbing Boundaries for Wave Propagation Problems* J. Comput. Phys. 63, 363-376 (1986)

[7] J. Mikusiński: *Operatorenrechnung*, Deutscher Verlag der Wissenschaften, Berlin (1957)

[8] F. Schmidt, P. Deuflhard: *Discrete Transparent Boundary Conditions for the Numerical Solution of Fresnel's Equation.* Computers Math. Applic. 29, pp. 53-76 (1995)

[9] D. Yevick, J. Yu, and Y. Yayon: *Optimal absorbing boundary conditions*, J. Opt. Soc. Am. A, vol. 12, 107-110 (1995)